doi.org/10.26434/chemrxiv.7250201.v1

Bioinspired Thiophosphorodichloridate Reagents for Chemoselective Histidine Bioconjugation

Shang Jia, Christopher Chang

Submitted date: 24/10/2018 • Posted date: 25/10/2018

Citation information: Jia, Shang; Chang, Christopher (2018): Bioinspired Thiophosphorodichloridate Reagents for Chemoselective Histidine Bioconjugation. ChemRxiv. Preprint.

Site-selective bioconjugation to native protein residues is a powerful tool for protein functionalization, with cysteine and lysine side chains being the most common points for attachment owing to their high nucleophilicity. We now report a strategy for histidine modification using thiophosphorodichloridate reagents that mimic post-translational histidine phosphorylation, enabling fast and selective labeling of protein histidines under mild conditions where various payloads can be introduced via copper-assisted alkyne-azide cycloaddition (CuAAC) chemistry. We establish that these reagents are particularly effective at covalent modification of His-tags, which are common motifs to facilitate protein purification, as illustrated by selective attachment of polyarginine cargoes to enhance the uptake of proteins into living cells. This work provides a starting point for probing and enhancing protein function using histidine-directed chemistry.

File list (2)

Bioinspired Thiophosphorodichloridate Reagents for Chemoselective Histidine Bioconjugation

Shang Jia[†] and Christopher J. Chang[†‡§*]

†Department of Chemistry, University of California, Berkeley, CA 94720, USA

‡Department of Molecular and Cell Biology, University of California, Berkeley, CA 94720, USA

§Howard Hughes Medical Institute, University of California, Berkeley, CA 94720, USA

Supporting Information Placeholder

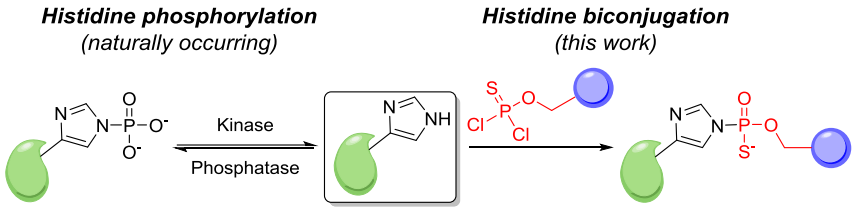

ABSTRACT: Site-selective bioconjugation to native protein residues is a powerful tool for protein functionalization, with cysteine and lysine side chains being the most common points for attachment owing to their high nucleophilicity. We now report a strategy for histidine modification using thiophosphorodichloridate reagents that mimic post-translational histidine phosphorylation, enabling fast and selective labeling of protein histidines under mild conditions where various payloads can be introduced via copper-assisted alkyne-azide cycloaddition (CuAAC) chemistry. We establish that these reagents are particularly effective at covalent modification of His-tags, which are common motifs to facilitate protein purification, as illustrated by selective attachment of polyarginine cargoes to enhance the uptake of proteins into living cells. This work provides a starting point for probing and enhancing protein function using histidine-directed chemistry.

INTRODUCTION

Site-selective bioconjugation chemistry offers a versatile strategy to probe and expand the function of proteins.[1–5] The most common and robust chemoselective and regioselective protein bioconjugation strategies have focused on functionalization of cysteine thiol [6–9] and lysine amine [10–12] sites and related nucleophilic hydroxyl [13,14] and carboxyl [15] side chains. More recent advances in protein bioconjugation technologies have targeted access to less nucleophlic amino acids,[16] including tyrosine,[17–19] tryptophan [20,21] and methionine.[22] In contrast, selective modification of histidine, which is commonly found in enzyme active sites and metal-binding sites,[23,24] remains underexplored. Because the imidazole side chain of histidine is a good metal ligand, metal coordination can enable protein modification through metal-directed covalent labeling proximal to the histidine group[25,26] or direct non-covalent metal-histidine complexation,[27–31] the latter of which can be labile under biological contexts or mass spectrometry conditions. On the other hand, histidine is a useful catalytic component owing to its ability to serve as both a good nucleophile and leaving group, but this character also makes it difficult to form stable bonds with the imidazole side chain through electrophilic functionalization. Indeed, selected epoxides are histidine-reactive but typically require harsh reaction conditions such as high temperatures and/or strong bases[32,33] or an affinity-directed ligand.[34,35] As such, selective and direct covalent labeling of histidine remains a challenge.

RESULTS AND DISCUSSION

Design and synthesis. Inspired by observations of reversible histidine phosphorylation as an emerging post-translational modification in prokaryotes and eukaryotes and elegant studies to probe its biological functions,[36–39] we sought to develop a histidine-selective bioconjugation method that mimics this type of chemistry (Figure 1a). We turned our attention to phosphorus-based electrophiles, based on precedent that potassium phosphoramidate can selectively phosphorylate histidine[40,41] and that thiophosphoryl chloride and potassium thiophosphoramidate can generate thiophosphohistidine analogs with improved aqueous stability.[42–44] To this end, we synthesized a series of phosphorus electrophiles with varying reactivity as suggested by their different synthesis and handling methods (Scheme 1). We first tested thiophosphoramidate **1** combining a phosphosulfide moiety for histidine labeling and an alkyne group for further functionalization, but this compound did not show an observable reaction with Fmoc-His-OH in buffered aqueous solution (Scheme 2). We then tested compound **2**, where we hypothesized that installation of chloride as a better leaving group might enhance reactivity. Indeed, thiophosphochloride **2** did show appreciable labeling of Fmoc-His-OH, but the resulting product underwent significant hydrolysis back to the unmodified histidine over prolonged

Scheme 1 Different routes for synthesis of phosphorus electrophiles.

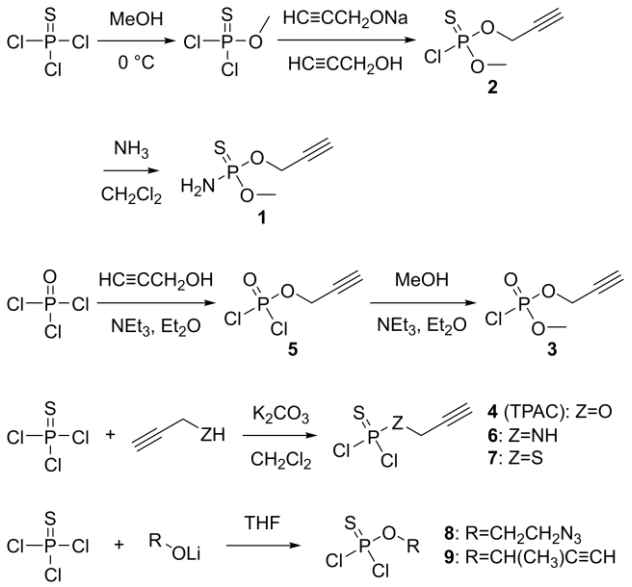

Scheme 2 Reaction yields of phosphorus electrophiles on Fmoc-His-OH.[a]

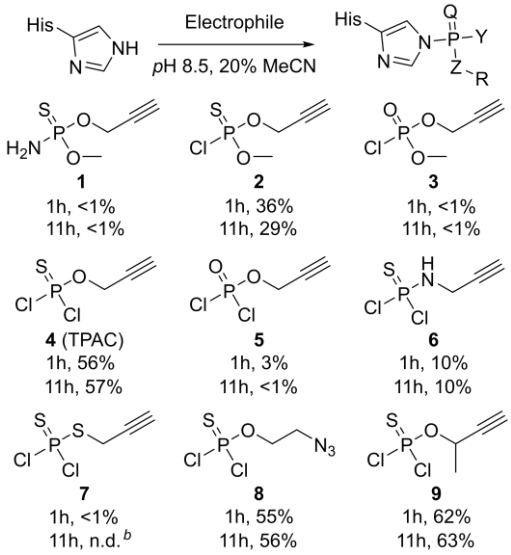

[a] Conditions: 0.5 mM Fmoc-His-OH, 5 mM electrophile, 25 mM HEPES *p*H 8.5, 20% MeCN, 1h; yields were determined by HPLC. [b] Reactant readily degenerates and forms precipitate.

incubation at neutral *p*H (Scheme 2), presumably due to the high acidity of the thiophosphoric acid diester as a leaving group.[45] To prevent this observed hydrolysis, we further replaced the methoxy group with another chloride that eventually hydrolyzes to the corresponding hydroxy congener to introduce a negative charge, akin to stable phosphate diester linkers found in nucleotides. The resulting compound **4**, termed thiophosphoro alkyne dichloridate (TPAC), gave higher conversion to product that is resistant to hydrolysis (Scheme 1, Table S1). The thiophosphorus electrophiles **2** and TPAC are superior histidine labeling reagents compared to their oxygen counterparts **3** and **5**, presumably owing to the greater stabilization provided by the less electronegative sulfur. The thiophosphodichloridate can be functionalized with other clickable handles such as azide **8** and sterically hindered alkyne **9** that show comparable reactivity. Further characterization using TPAC as a representative thiophosphodichloridate reagents shows optimal histidine labeling at more basic *p*H values, affording a 60% yield of bioconjugate within twenty minutes at *p*H 8.5 (Figure 1b). The short observed reaction time for TPAC-mediated histidine labeling is primarily controlled by the fast hydrolysis of TPAC itself (Figure S1), which is

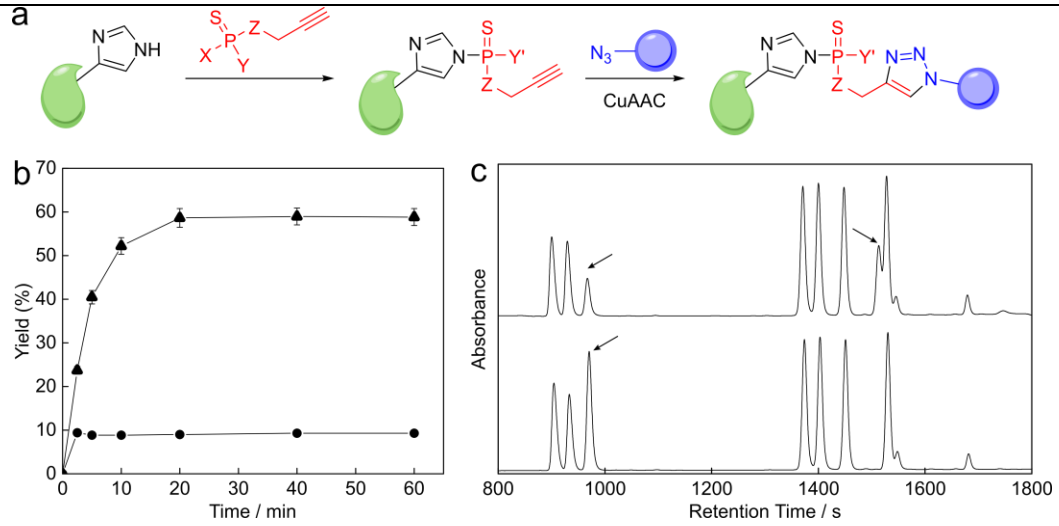

Figure 1 Labelling of histidine with phosphorus electrophiles. (a) Scheme of histidine labeling and the following click reaction for bioconjugation. X, Y=Cl, OH, OMe or NH_2, Z=O, NH or S. (b) Kinetics of reaction between TPAC and Fmoc-His-OH. Triangle: *p*H 8.5. Circle: *p*H 7.5. (n=3, average ±s.d.). (c) HPLC chromatograph showing the reaction between TPAC and Fmoc-His-OH in the presence of competing Fmoc-protected amino acids. Top: reaction mixture of TPAC and amino acids. Bottom: amino acids mixture; left to right: Fmoc-Lys, Fmoc-Arg, Fmoc-His, Fmoc-Ser, Fmoc-Glu, Fmoc-Thr and Fmoc-Tyr. Arrows point to Fmoc-His-OH (left) and TPAC-labelled Fmoc-His-OH (right, ESI-MS m/z expected 512.1, found 512.2 for $M+H^+$).

advantageous since the reaction does not require quenching of residual TPAC to halt its reactivity and the reagent can thus be used in excess. Moreover, the thiophospho-histidine product shows reasonable stability under various conditions including high temperature, acidic, basic, reducing and alkylating environments (Table S1). Most importantly, TPAC exhibits high selectivity for histidine, showing negligible reactivity on other nucleophilic amino acids (Figure 1c, Figure S2). The results collectively identify TPAC as a promising candidate for chemoselective bioconjugation to histidine.

TPAC bioconjugation on model proteins. With these results in hand, we moved on to test TPAC labeling of histidine on intact protein substrates (Figure 1a). We used ribonuclease A as a model protein and analyzed bioconjugation reactions by mass spectrometry. The TPAC labeling is dose-dependent, generating ca. 45% singly-modified protein and 11% doubly-modified protein at *p*H 8.5 (Figure 2b). Similar to what was observed in small-molecule amino acid models, the TPAC-ribonuclease A coupling reaction was more effective at slightly basic conditions compared to neutral *p*H (Figure 2c). We further performed LC-MS/MS of the digested protein to analyze the site of modification. Similar to other phosphopeptides, the TPAC modification undergoes significant neutral loss in collision-induce dissociation (CID), but the fragment peaks are sufficient for identifying the site of modification (Figure S3d−e). We also used electron-transfer dissociation (ETD) on peptides with ambiguous modification sites for supplementary information (Figure S3c). Interestingly, the LC-MS/MS of the digested protein indicates that the reaction occurs primarily on H48, a surface-exposed histidine rather than histidines at the catalytic center (H12 and H119). In addition, two other histidine sites, on at the active site (H119) and one that is not (H105), are also modified to less extent, as shown qualitatively by extracted precursor ion chromatogram (Figure S3a). The data are also in line with the negligible loss of activity of ribonuclease A after TPAC treatment (Figure S3b).

We then demonstrated that the TPAC bioconjugation method is amenable to labeling histidine residues on other proteins, including calmodulin, myoglobin and lysozyme. The yields vary for these proteins (Figure 2d−f), and the reaction shows excellent histidine selectivity on calmodulin and myoglobin (Figure S4, S5). Modest side-reactivity towards lysine is observed on lysozyme, but lysine labeling can be suppressed by lowering the *p*H to 7.5 to further block the nucleophilicity of the lysine residues by protonation, while increasing TPAC concentrations to compensate the decreased histidine reactivity (Figure S6). TPAC labeling in HeLa lysates also proceeds smoothly as shown by in-gel fluorescence (Figure S7a), and more importantly, pretreatments of lysates with competing electrophiles that block cysteine, lysine or serine residues do not affect the observed TPAC signal, suggesting that the reagent does not appreciably react with these competing amino acid residues (Figure S7b-e). Taken together, the results show that TPAC is effective at selectively labeling native histidine residues on proteins.

We then sought to apply this histidine bioconjugation method to install clickable payloads onto proteins. Considering that TPAC converts the slightly basic histidine residue into a rather acidic thiophosphoric acid derivative, we reasoned that the labeled protein can be separated readily from the unreacted

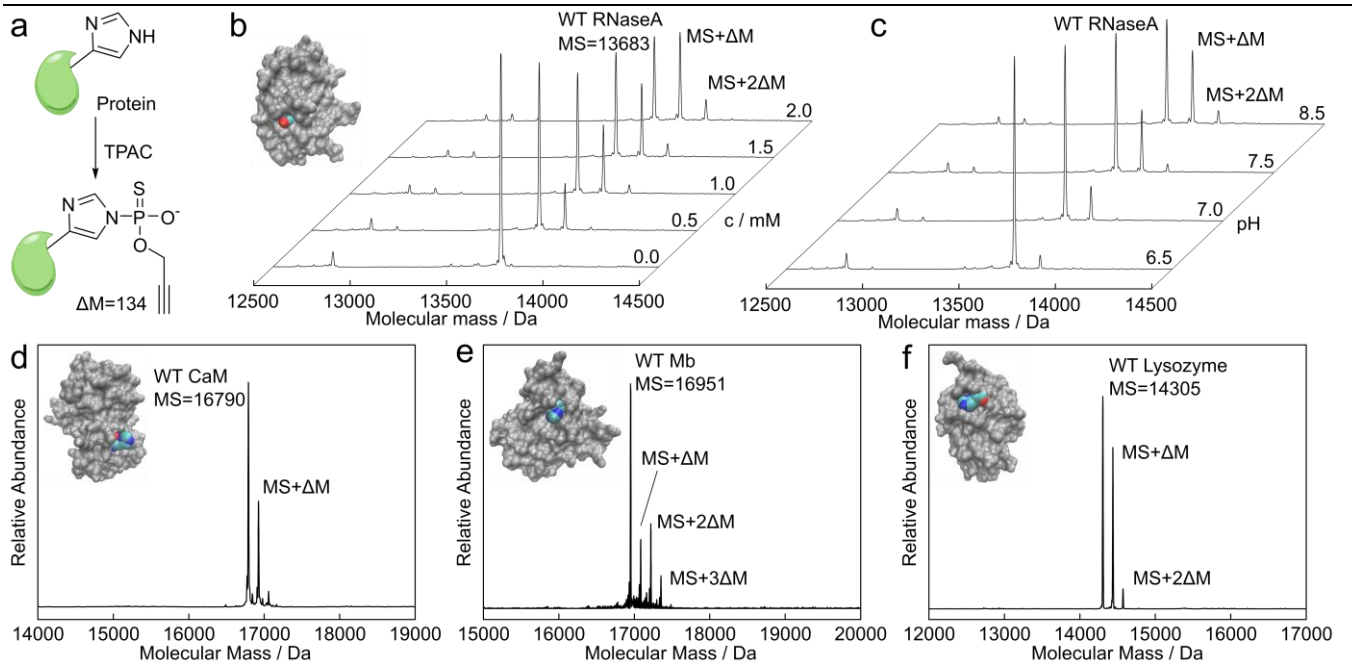

Figure 2 Model protein tagging with TPAC. (a) Structure and mass difference of the histidine modification by TPAC. (b) Deconvoluted mass spectra showing ribonuclease A labelled by TPAC with concentration ranging from 0 to 2 mM. Single and double TPAC modified RNaseA: expected mass 13817, 13951 Da, found 13816, 13950 Da. Its crystal structure (PDB 1bel) is shown in the inset highlighting its major modified histidine. (c) Deconvoluted mass spectra showing ribonuclease A labelled with 1.5 mM of TPAC with different buffered *p*H. (d) Calmodulin, (e) myoglobin and (f) lysozyme are also labelled by TPAC as shown by their deconvoluted mass spectra. TPAC-modified calmodulin: expected mass 16924 Da, found 16924 Da; single, double and triple TPAC modified myoglobin: expected mass 17085, 17219 and 17353 Da, found 17085, 17218 and 17352 Da; single and double TPAC modified lysozyme: expected mass 14439, 14573 Da, found 14438, 14572 Da. Their crystal structures (PDB 2o60, 1bje and 193l) are shown as insets highlighting the major modified histidines. Conditions: 20 μM protein, 2 mM TPAC in 25 mM HEPES with *p*H 8.5, room temperature, 1 h unless otherwise noted.

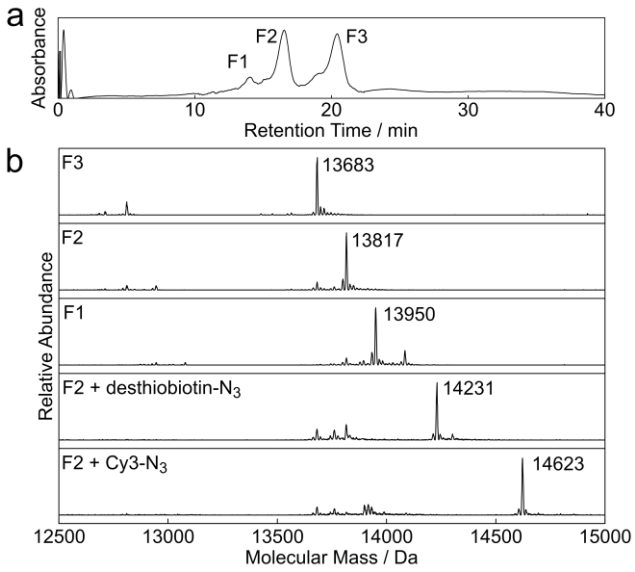

Figure 3 Protein bioconjugation with TPAC. (a) Chromatogram at 280 nm showing the separation of the reaction mixture between ribonuclease A and TPAC by strong cation exchange column. Three fractions, F1-3, were collected for analysis. (b) Deconvoluted mass spectra of ribonuclease A in F1-3, and TPAC-modified ribonuclease A in F2 reacted with the model azide compounds by CuAAC. Found masses are labelled next to the peak. Expected masses for non-, single- and double-labelled ribonuclease A are 13683, 13817, 13951 Da, respectively. Expected masses for single TPAC/desthiobiotin-N_3 and TPAC/Cy3-N_3 labelled ribonuclease A are 14231 and 14623 Da, respectively.

protein by its charge difference. Indeed, the separation of the reaction mixture of ribonuclease A and TPAC is effective on a strong cation exchange column buffered at *p*H 4.2, giving rise to three fractions (Figure 3a). The mass spectra of these fractions confirms our hypothesis: unreacted ribonuclease A carries more positive charge and elutes last, the doubly TPAC-modified ribonuclease A protein is less positively charged and elutes first, and the singly TPAC-modified protein elutes between these two fractions (Figure 3b). After the facile isolation of TPAC-modified reaction products, we further performed copper(I)-catalyzed alkyne-azide cycloaddition (CuAAC) between mono-labeled ribonuclease A and either Cy3-N_3 or desthiobiotin-N_3 payloads for detection and enrichment, respectively (Figure S8). As expected, the obtained protein is uniform with only one payload per protein molecule (Figure 3b). Collectively, TPAC labeling with subsequent ion exchange chromatography and CuAAC chemistry provides a versatile and robust workflow to create homogenous proteins modified on histidine residues.

TPAC bioconjugation on His-tag for protein delivery. To showcase the potential merits of TPAC bioconjugation chemistry at the cellular level, we turned our attention to selective modification of polyhistidine-tagged proteins (e.g., His-tag). His-tag is a widely used method for purification of proteins by introducing a short polyhistidine peptide fused to the surface exposed portion of the protein of interest for sub-sequent resin capture and separation. We envisioned that this polyhistidine motif would greatly enhance the labeling efficiency of TPAC in a site-specific manner, and we demonstrated this possibility by combining TPAC labeling with further bioconjugation by CuAAC with polyarginine, a cell-penetrating peptide, to create a general method for enabling protein delivery into living cells (Figure 4a). We utilized GFP bearing an N-terminal 10×His-

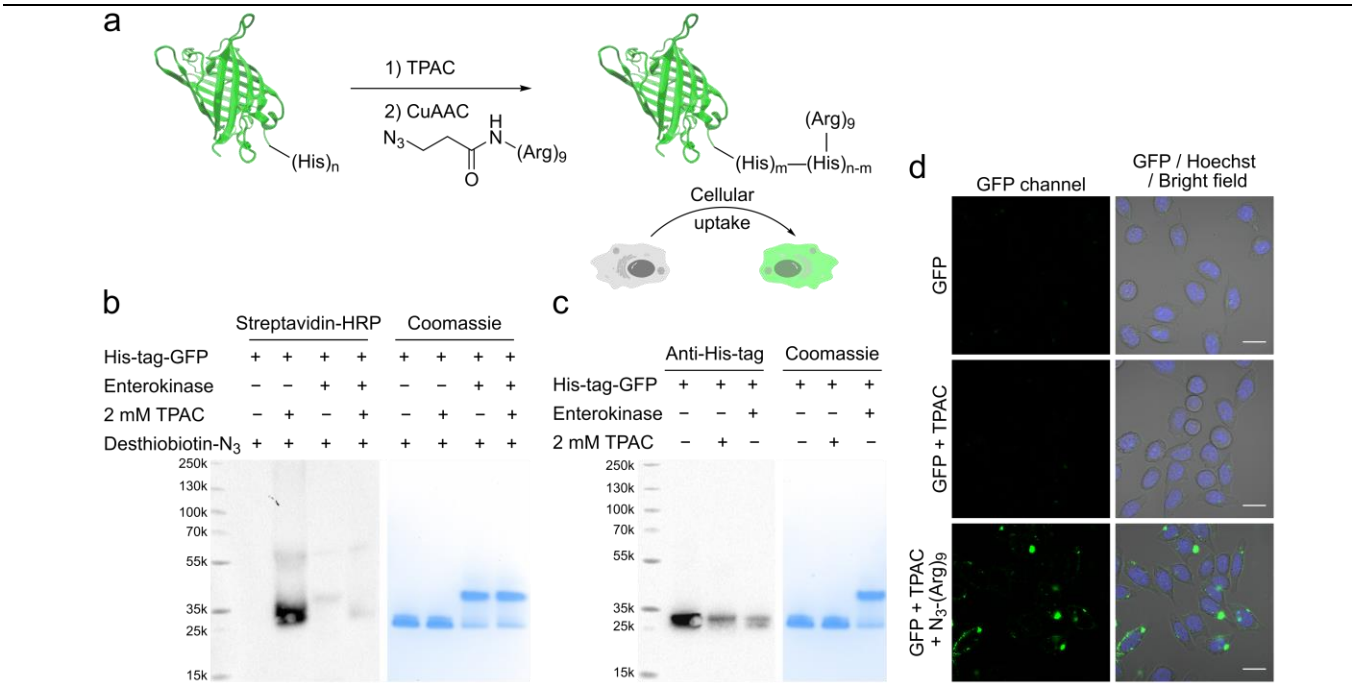

Figure 4 Functionalization of His-tag on GFP to enable protein delivery. (a) Scheme of bioconjugation of polyarginine onto His-tag of a fluorescent protein using TPAC. (b) Streptavidin-HRP blot and coomassie stain showing that removal of the His-tag significantly reduces the labeling by TPAC. His-tagged GFP and native GFP prepared by enterokinase cleavage of His-tag were treated with TPAC, followed by CuAAC with desthiobiotin-N_3 and gel-analysis. Cleavage of His-tag leads to less coomassie staining but with similar migration on SDS-PAGE (Figure S11a). (c) Western blot and coomassie stain showing that labelling of TPAC with His-tagged GFP significantly reduces its detection by His-tag antibody. (d) Transduction of functionalized GFP into live HeLa cells. Cells were incubated with GFP (0.1 μg/μL), stained with Hoechst 33342 and imaged. Scale-bars: 20 μm.

tag as a proof-of-concept protein, where TPAC-labeling greatly reduces binding and recognition of His-tag GFP by a His-tag antibody, consistent with efficient labeling of TPAC in this His-tag region (Figure 4c). Indeed, TPAC labeling followed by CuAAC with desthiobiotin-N_3 on His-tag GFP produces a significantly stronger signal compared to GFP without the His-tag on a streptavidin blot (Figure 4b), further indicating that TPAC selectively reacts with histidine residues on the His-tag rather than other histidine residues on this protein. Similarly, LC-MS analysis of the digested protein after TPAC treatment only identifies one to three modifications, all of which appear on the His-tag region (Figure S9). With this information in hand, we performed CuAAC between TPAC-labeled His-tag GFP and N_3-$(Arg)_9$-OH to introduce cell-penetrating capabilities onto the protein. Indeed, the $(Arg)_9$-functionalized GFP is now capable of being delivered into HeLa cells as shown by increases in intracellular green fluorescence as observed by confocal microscopy, whereas His-tagged GFP without TPAC or N_3-$(Arg)_9$-OH treatment results in no fluorescence signal over dark background (Figure 4d). Similar results are also observed with an mCherry construct carrying an N-terminus 6×His-tag (Figure S10). Taken together, this line of experiments shows that TPAC can provide covalent, histidine-selective bioconjugation that is functional in living cells.

CONCLUSION

To close, we have reported thiophosphorodichloridates inspired by native histidine phosphorylation processes as reagents for histidine-selective covalent modification of proteins. With TPAC, an alkyne-tagged version of this family of probes, we demonstrated efficient bioconjugation on model proteins with excellent selectivity for histidine over other potentially reactive amino acids. TPAC-labeled proteins are readily purified and can undergo further coupling with bioorthogonal click chemistry to introduce a variety of payloads. In one example to illustrate the utility of this approach, TPAC labeling was applied to introduce polyarginine motifs selectively onto His-tag proteins to endow membrane permeability and enable delivery into living cells. Owing to central importance of histidine residues in enzyme chemistry, this work provides a new type of reagent for probing histidine function in native contexts. Likewise, the efficient labeling of polyhistidine tags can enable versatile protein functionalization for biochemical and protein engineering studies in both fundamental and applied settings. Coupled with recent work from our laboratory on the development of selective methionine bioconjugation reagents that operate by redox-mediated nitrogen group transfer processes inspired by native oxygen atom-transfer oxidations that transform methionine to methionine sulfoxide,[22] mimicking histidine phosphorylation can provide a starting point for developing histidine-selective bioconjugation chemistry. We are currently expanding and applying the toolbox of activity-based sensing reagents in this direction to develop chemoselective probes for other reactive amino acid sites in proteins and proteomes.

Experimental Section

Chemical and protein materials. All commercial reagents were used without further purification. Fmoc-Cys-OH was purchased from Chem-Impex (Wood Dale IL). All other Fmoc-protected amino acids were purchased from Ark Pharm (Arlington Heights IL). 2-(4-((bis((1-(tert-butyl)-1H-1,2,3-triazol-4-yl)methyl)amino)methyl)-1H -1,2,3-triazol-1-yl)acetic acid (BTTAA) was purchased from Click Chemistry Tools (Scottsdale AZ). Ribonuclease A from bovine pancreas, lyzome from chicken egg white, myoglobin from equine heart and all other chemicals were purchased from Sigma-Aldrich (St. Louis MO). Calmodulin, porcine was purchased from rPeptide (Watkinsville GA). His-tagged GFP was purchased from Sino Biological (Beijing, China). His-tagged mCherry was purchased from Origene (Rockville MD). Enterokinase was purchased from New England Biolabs (Ipswich MA). TEV protease was purchased from QB3 (San Francisco CA). Enzymes were used following the protocols provided by their manufacturer.

Reaction between phosphorus electrophiles and amino acids. Fmoc-protected amino acid was dissolved in DMSO (100 mM) and diluted to a final concentration of 0.5 mM in 25 mM HEPES buffer, *p*H 8.5 containing 20% MeCN unless otherwise noted. To this solution was added 5 mM of phosphorus electrophile (50x stock in MeCN). The reaction was performed at room temperature for 1 h unless otherwise noted, filtered and immediately subject to LC/MS analysis. For reaction with Fmoc-protected amino acid mixtures, 0.3 mM of each protected amino acid in 50 mM HEPES buffer, *p*H 8.5 containing 20% MeCN was reacted with 3 mM of TPAC.

Protein labelling with TPAC. Proteins were diluted into 25 mM HEPES, *p*H 8.5 to a concentration of 20 μM unless otherwise noted. Samples were labelled with 2 mM of TPAC (50x stock in MeCN). The reaction was performed at room temperature for 1 h. Samples were then subject to LC/MS analysis or further click reaction or LC-MS analysis.

Purification of TPAC-labelled ribonuclease A. The reaction mixture of RNase A with TPAC was diluted in 20 mM sodium succinate, *p*H 4.2 and was loaded onto HiTrap SP HP cation exchange chromatography column (1 mL, GE Healthcare, Chicago IL). The protein was then separated with a linear gradient from 20 mM sodium succinate, *p*H 4.2 to 25 mM succinate with 1 M NaCl, *p*H 4.2 at a flow rate of 1.0 mL/min over 40 min. The collected fractions were concentrated and buffer-exchanged into desired buffer for click reaction or LC/MS analysis.

Click reactions on TPAC-labelled proteins. We followed the protocol recommended by M. Finn, *et al* for click reactions.[46] Namely, protein solution in HEPES or PBS buffer was treated with 1 mM aminoguanidine hydrochloride (100x stock in water), 100 μM $CuSO_4$ (100x stock in water), 500 μM THPTA or BTTAA (100x stock in water), 100 μM organic azide (100x stock in DMSO or water) and 5 mM sodium ascorbate (100x stock in water). For reaction on his-tagged protein 100 μM $NiCl_2$ (100x stock in water) was also added. The reaction was mixed thoroughly and placed in the dark at room temperature. After 1 h the reaction was quenched by adding 500 μM EDTA.

For click reaction with Cy3-N_3, proteins were precipitated with acetone prior to click reaction to remove excess TPAC. The pellet was dissolved in PBS containing 0.1% SDS for click reaction, and precipitated again to remove unreacted dye. The pellet was then dissolved in running buffer and analyzed by SDS-PAGE.

For click reaction on TPAC-labelled, His-tagged proteins, proteins were buffer-exchanged into 25 mM HEPES, *p*H 7.5 by extensive ultrafiltration (Amnicon 10K, EMD Millipore, Hayward CA) prior to click reaction. After the click reaction, proteins were buffer-exchanged into PBS by extensive ultrafiltration to remove unwanted chemicals.

Cell culture and imaging Cells were grown in the Cell Culture Facility at the University of California, Berkeley. HeLa cells were cultured in DMEM supplemented with 10% FBS and glutamine (2 mM). One day before imaging, cells were passed and plated on eight-well chamber slides (Lab-Tek, Thermo Fisher).

For imaging, cells were grown on 8-well chamber slides (LabTek, Thermo Fisher) to desired confluency, washed with PBS and incubated with 0.1 mg/mL $(Arg)_9$-labelled GFP or mCherry in PBS for 15 min at 37 ℃. The cells were then washed with PBS and stained with 1 μM Hoechst 33342 for 15 min, washed again and imaged on a Zeiss LSM710 laser-scanning microscope with a 63× oil-immersion objective lens. Excitation was provided at 405 for Hoechst 33342, 488 nm for GFP and 543 nm for mCherry.

Synthesis of methyl propargyl thiophosphorochloridate (2). To a flask containing $PSCl_3$ (2 mL, 20 mmol) cooled in ice/water bath was added dry methanol (2.0 mL, 49 mmol) dropwise. The mixture was stirred for 15 min on ice and excess methanol was distilled under vacuum at the same temperature to give crude methyl thiophosphorodichloridate. Sodium (0.453 g, 19.7 mmol) was dissolved in cooled propargyl alcohol (6.0 mL, 104 mmol) to form an orange, thick solution, which was added dropwise to methyl thiophosphorodichloridate cooled in ice/water bath. The suspension was further stirred for 2 h at room temperature, diluted with CH_2Cl_2, filtered and purified by column chromatography (30:1 hexanes/EtOAc) to give product 2 as a colorless oil (2.4 g, 67%). ^{1}H NMR (400 MHz, $CDCl_3$) δ 4.85 – 4.80 (m, 2H), 3.91 (d, *J* = 16.1 Hz, 3H), 2.63 (t, *J* = 2.5 Hz, 1H). ^{13}C NMR (101 MHz, $CDCl_3$) δ 77.16, 76.45, 76.34, 56.92, 56.88, 56.01, 55.94. ^{31}P NMR (162 MHz, $CDCl_3$) δ 71.91. HRMS ($APCI^+$) m/z calcd 184.9587, found 184.9586 for $C_4H_7ClO_2PS^+$ ($M+H^+$).

Synthesis of methyl propargyl thiophosphoramidate (1). Crude **2** in propargyl alcohol and CH_2Cl_2 was prepared as described above. Excess ammonia was led through this mixture to form NH_4Cl as a precipitate. The mixture was filtered, concentrated and purified by column chromatography (2:1 hexanes/EtOAc) to give product **1** as a light yellow oil (2.1 g, 65% overall yield). ^{1}H NMR (400 MHz, MeOD) δ 4.62 (dd, *J* = 10.5, 2.5 Hz, 2H), 3.68 (d, *J* = 13.8 Hz, 3H), 2.94 (t, *J* = 2.5 Hz, 1H). ^{13}C NMR (101 MHz, MeOD) δ 79.52, 79.41, 76.35, 55.05, 55.02, 53.75, 53.70. ^{31}P NMR (162 MHz, MeOD) δ 78.25. HRMS ($APCI^+$) m/z calcd 166.0086, found 166.0097 for $C_4H_9NO_2PS^+$ ($M+H^+$).

Synthesis of propargyl thiophosphorodichloridate (4, TPAC). To a solution of $PSCl_3$ (1.0 mL, 9.8 mmol) in CH_2Cl_2 (10 mL) was added propargyl alcohol (0.57 mL, 9.8 mmol) and K_2CO_3 (1.36 g, 9.8 mmol). After overnight stirring at room temperature, the mixture was filtered and purified by column chromatography (50:1 hexanes/EtOAc) to give product **TPAC** as a colorless oil with a pungent smell (1.1 g, 55%). ^{1}H NMR (400 MHz, $CDCl_3$) δ 4.94 (dd, *J* = 15.9, 2.5 Hz, 2H), 2.72 (t, *J* = 2.5 Hz, 1H). ^{13}C NMR (101 MHz, $CDCl_3$) δ 78.37, 75.53, 75.42, 58.56, 58.48. ^{31}P NMR (162 MHz, $CDCl_3$) δ 59.68. HRMS ($APCI^+$) m/z calcd 188.9092, found 188.9115 for $C_3H_4Cl_2OPS^+$ ($M+H^+$).

Synthesis of propargyl phosphorodichloridate (5). $POCl_3$ (1.0 mL, 11 mmol) and propargyl alcohol (0.62 mL, 11 mmol) was dissolved in Et_2O (20 mL) and cooled in dry ice/acetone bath under N_2. Triethylamine (1.5 mL, 11 mmol) was dissolved in Et_2O (20 mL) and added dropwise via addition funnel to form a white suspension. The reaction mixture was warmed to room temperature and was furthered stirred at room temperature for 2 h. Trimethylamine hydrochloride was removed by filtration, and the solution was concentrated to give product **5** as a light yellow oil with a pungent smell (1.8 g, 99%). The product was used without further purification. ^{1}H NMR (400 MHz, $CDCl_3$) δ 4.92 (dd, *J* = 14.5, 1.0 Hz, 2H), 2.76 (t, *J* = 1.0 Hz 1H). ^{1}H NMR (400 MHz, $CDCl_3$) δ 4.94, 4.94, 4.90, 4.90, 3.48, 3.46, 2.76, 1.21, 1.19, 1.17. ^{13}C NMR (101 MHz, $CDCl_3$) δ 78.93, 74.96, 74.86, 58.56, 58.49. ^{31}P NMR (162 MHz, $CDCl_3$) δ 8.70. LRMS (EI^+) m/z calcd 137.0, found 136.9 for $C_3H_3ClO_2P^+$ ($M-Cl^-$).

Synthesis of methyl propargyl phosphorochloridate (3). Crude **5** with trimethylamine hydrochloride in Et_2O was prepared as described above. The mixture was cooled again in dry ice/acetone bath. Dry methanol (0.43 mL, 11 mmol) and trimethylamine (1.5 mL, 11 mmol) in Et_2O (20 mL) was added dropwise via addition funnel. The slurry was further stirred at room temperature for 3 h, filtered and concentrated to give product **3** as light yellow oil with a pungent smell (1.7 g, 93%). ^{1}H NMR (400 MHz, $CDCl_3$) δ 4.79 (dd, *J* = 11.5, 2.5 Hz, 1H), 3.92 (d, *J* = 13.8 Hz, 3H), 2.66 (t, *J* = 2.5 Hz, 1H). ^{13}C NMR (101 MHz, $CDCl_3$) δ 78.92, 76.09, 76.00, 56.68, 56.63, 56.01, 55.94. ^{31}P NMR (162 MHz, $CDCl_3$) δ 6.74. HRMS ($APCI^+$) m/z calcd 168.9816, found 168.9855 for $C_4H_7ClO_3P^+$ ($M+H^+$).

Synthesis of *N*-propargyl thiophosphoramidic dichloride (6). To a solution of $PSCl_3$ (0.30 mL, 2.9 mmol) in CH_2Cl_2 (5 mL) was added propargyl amine (0.19 mL, 2.9 mmol) and K_2CO_3 (0.41 g, 2.9 mmol). After 2 h stirring at room temperature, the mixture was filtered and purified by column chromatography (30:1 hexanes/EtOAc) to give product **6** as a yellow oil with a pungent smell (0.25 g, 49%). ^{1}H NMR (400 MHz, Acetone) δ 4.09 (dd, *J* = 20.7, 2.5 Hz, 2H), 2.89 (t, *J* = 2.5 Hz, 1H). ^{13}C NMR (101 MHz, Acetone) δ 79.94, 79.85, 74.13, 33.42. ^{31}P NMR (162 MHz, Acetone) δ 57.59. HRMS (EI^+) m/z calcd 151.9, found 152.0 for $C_3H_4ClNPS^+$ ($M-Cl^-$).

Synthesis of propargyl dithiophosphorodichloridate (7). *S*-propargyl thioacetate (0.35 mg, 3.1 mmol) was stirred with NaOH (0.16 g, 4.0 mmol) in MeOH (10 mL) under N_2 for 30 min. The mixture was then diluted with CH_2Cl_2 (30 mL), washed with H_2O (×4) and dried (Na_2SO_4). To this solution was added $PSCl_3$ (0.37 mL, 3.7 mmol) and K_2CO_3 (0.51g, 3.7 mmol) and the mixture was stirred overnight. The mixture was filtered and purified by column chromatography (100:1 hexanes/EtOAc) to give product **7** as a light yellow oil, which degenerates into a solid mixture soon after concentration. ^{1}H NMR (600 MHz, $CDCl_3$) δ 3.75 (dd, *J* = 15.6, 2.7 Hz, 2H), 2.35 (t, *J* = 2.7 Hz, 1H).

Synthesis of 2-azidoethyl thiophosphorodichloridate 8. 2-Azidoethanol (0.43 g, 4.9 mmol) was dissolved in dry THF (15 mL) under N_2 and cooled in dry ice/acetone bath. To this solution was added dropwise *n*BuLi (2.0 mL, 2.5 M in hexanes) and stirred for 20 min at room temperature to form the lithium salt. To another flask cooled in dry ice/acetone bath was added THF (15 mL) and $PSCl_3$ (1.0 mL, 4.9 mmol) under N_2. The lithium salt solution was then added dropwise at this temperature and the mixture was then stirred for 1h at room temperature. The mixture was concentrated, diluted in CH_2Cl_2, filtered to remove lithium chloride and purified by column chromatography (50:1 hexanes/EtOAc) to give product **8** as a light yellow oil with a pungent smell (0.60 g, 56%). ^{1}H NMR (400 MHz, $CDCl_3$) δ 4.45 (dt, *J* = 11.0, 5.1 Hz, 2H), 3.63 (t, *J* = 4.4 Hz, 2H). ^{13}C NMR (101 MHz, $CDCl_3$) δ 69.62, 69.52, 50.16, 50.06. ^{31}P NMR (162 MHz, $CDCl_3$) δ 59.05. HRMS

(APCI$^+$) m/z calcd 191.9202, found 191.9219 for $C_2H_5Cl_2NOPS^+$ ($M-N_2+H^+$).

Synthesis of (±)-3-butyn-2-yl thiophosphorodichloridate (9). (±)-3-Butyn-2-ol (0.77 mL, 9.8 mmol) was dissolved in dry THF (10 mL) under N_2 and cooled in dry ice/acetone bath. To this solution was added dropwise *n*BuLi (3.9 mL, 2.5 M in hexanes) and stirred for 20 min at room temperature to form the lithium salt. To another flask cooled in dry ice/acetone bath was added THF (20 mL) and $PSCl_3$ (1.0 mL, 9.8 mmol) under N_2. The lithium salt solution was then added dropwise at this temperature and the mixture was then stirred for 3h at room temperature. The mixture was concentrated, diluted in CH_2Cl_2, filtered to remove lithium chloride and purified by column chromatography (100:1 hexanes/EtOAc) to give product **9** as a colorless oil with a pungent smell (0.53 g, 26%). ^{1}H NMR (400 MHz, $CDCl_3$) δ 5.46 (dqd, *J* = 13.3, 6.6, 2.1 Hz, 1H), 2.71 (d, *J* = 2.2 Hz, 1H), 1.71 (dd, *J* = 6.6, 0.8 Hz, 3H). ^{13}C NMR (101 MHz, $CDCl_3$) δ 79.99, 79.92, 76.64, 69.25, 69.16, 23.21, 23.14. ^{31}P NMR (162 MHz, $CDCl_3$) δ 58.98. HRMS (APCI$^+$) m/z calcd 202.9249, found 202.9261 for $C_4H_6Cl_2OPS^+$ ($M+H^+$).

ASSOCIATED CONTENT

Supporting Information

Supplementary experimental materials and analytical methods, supplementary reaction characterization, summary of LC-MS/MS results, analysis of bioconjugation on cell lysate and mCherry protein, supplementary synthesis and characterization (PDF)

AUTHOR INFORMATION

Corresponding Author

*Phone: 001-(510)642-4704. E-mail: chrischang@berkeley. edu. Twitter: @christhechang.

Notes

The authors declare no competing financial interest.

ACKNOWLEDGMENT

We thank the National Institutes of Health (ES 028096), Novartis Institutes for BioMedical Research and the Novartis-Berkeley Center for Proteomics and Chemistry Technologies (NB-CPACT) for supporting this work. C.J.C. is an investigator of the Howard Hughes Medical Institute. We thank Dr. Dan He (University of California, Berkeley) for helpful suggestions. The QB3/Chemistry Mass Spectrometry Facility at the University of California, Berkeley received support from National Institutes of Health (grant 1S10OD020062-01).

REFERENCES

(1) Stephanopoulos, N.; Francis, M. B. Choosing an Effective Protein Bioconjugation Strategy. *Nat. Chem. Biol.* **2011**, *7* (12), 876–884.

(2) Spicer, C. D.; Davis, B. G. Selective Chemical Protein Modification. *Nat. Commun.* **2014**, *5*, 4740.

(3) McKay, C. S.; Finn, M. G. Click Chemistry in Complex Mixtures: Bioorthogonal Bioconjugation. *Chem. Biol.* **2014**, *21* (9), 1075–1101.

(4) Koniev, O.; Wagner, A. Developments and Recent Advancements in the Field of Endogenous Amino Acid Selective Bond Forming Reactions for Bioconjugation. *Chem. Soc. Rev.* **2015**, *44* (15), 5495–5551.

(5) Boutureira, O.; Bernardes, G. J. L. Advances in Chemical Protein Modification. *Chem. Rev.* **2015**, *115* (5), 2174–2195.

(6) Vinogradova, E. V.; Zhang, C.; Spokoyny, A. M.; Pentelute, B. L.; Buchwald, S. L. Organometallic Palladium Reagents for Cysteine Bioconjugation. *Nature* **2015**, *526* (7575), 687–691.

(7) Zhang, C.; Welborn, M.; Zhu, T.; Yang, N. J.; Santos, M. S.; Voorhis, T. V.; Pentelute, B. L. π-Clamp-Mediated Cysteine Conjugation. *Nat. Chem.* **2016**, *8* (2), 120–128.

(8) Willwacher, J.; Raj, R.; Mohammed, S.; Davis, B. G. Selective Metal-Site-Guided Arylation of Proteins. *J. Am. Chem. Soc.* **2016**, *138* (28), 8678–8681.

(9) Messina, M. S.; Stauber, J. M.; Waddington, M. A.; Rheingold, A. L.; Maynard, H. D.; Spokoyny, A. M. Organometallic Gold(III) Reagents for Cysteine Arylation. *J. Am. Chem. Soc.* **2018**, *140* (23), 7065–7069.

(10) Matos, M. J.; Oliveira, B. L.; Martínez-Sáez, N.; Guerreiro, A.; Cal, P. M. S. D.; Bertoldo, J.; Maneiro, M.; Perkins, E.; Howard, J.; Deery, M. J.; et al. Chemo- and Regioselective Lysine Modification on Native Proteins. *J. Am. Chem. Soc.* **2018**, *140* (11), 4004–4017.

(11) Ward, C. C.; Kleinman, J. I.; Nomura, D. K. NHS-Esters As Versatile Reactivity-Based Probes for Mapping Proteome-Wide Ligandable Hotspots. *ACS Chem. Biol.* **2017**, *12* (6), 1478–1483.

(12) Hacker, S. M.; Backus, K. M.; Lazear, M. R.; Forli, S.; Correia, B. E.; Cravatt, B. F. Global Profiling of Lysine Reactivity and Ligandability in the Human Proteome. *Nat. Chem.* **2017**, *9* (12), 1181–1190.

(13) Liu, Y.; Patricelli, M. P.; Cravatt, B. F. Activity-Based Protein Profiling: The Serine Hydrolases. *Proc. Natl. Acad. Sci.* **1999**, *96* (26), 14694–14699.

(14) Kidd, D.; Liu, Y.; Cravatt, B. F. Profiling Serine Hydrolase Activities in Complex Proteomes. *Biochemistry (Mosc.)* **2001**, *40* (13), 4005–4015.

(15) McGrath, N. A.; Andersen, K. A.; Davis, A. K. F.; Lomax, J. E.; Raines, R. T. Diazo Compounds for the Bioreversible Esterification of Proteins. *Chem. Sci.* **2014**, *6* (1), 752–755.

(16) deGruyter, J. N.; Malins, L. R.; Baran, P. S. Residue-Specific Peptide Modification: A Chemist's Guide. *Biochemistry (Mosc.)* **2017**, *56* (30), 3863–3873.

(17) Schlick, T. L.; Ding, Z.; Kovacs, E. W.; Francis, M. B. Dual-Surface Modification of the Tobacco Mosaic Virus. *J. Am. Chem. Soc.* **2005**, *127* (11), 3718–3723.

(18) Romanini, D. W.; Francis, M. B. Attachment of Peptide Building Blocks to Proteins Through Tyrosine Bioconjugation. *Bioconjug. Chem.* **2008**, *19* (1), 153–157.

(19) Ban, H.; Gavrilyuk, J.; Barbas, C. F. Tyrosine Bioconjugation through Aqueous Ene-Type Reactions: A Click-Like Reaction for Tyrosine. *J. Am. Chem. Soc.* **2010**, *132* (5), 1523–1525.

(20) Antos, J. M.; Francis, M. B. Selective Tryptophan Modification with Rhodium Carbenoids in Aqueous Solution. *J. Am. Chem. Soc.* **2004**, *126* (33), 10256–10257.

(21) Antos, J. M.; McFarland, J. M.; Iavarone, A. T.; Francis, M. B. Chemoselective Tryptophan Labeling with Rhodium Carbenoids at Mild PH. *J. Am. Chem. Soc.* **2009**, *131* (17), 6301–6308.

(22) Lin, S.; Yang, X.; Jia, S.; Weeks, A. M.; Hornsby, M.; Lee, P. S.; Nichiporuk, R. V.; Iavarone, A. T.; Wells, J. A.; Toste, F. D.; et al. Redox-Based Reagents for Chemoselective Methionine Bioconjugation. *Science* **2017**, *355* (6325), 597–602.

(23) Gutteridge, A.; Thornton, J. M. Understanding Nature's Catalytic Toolkit. *Trends Biochem. Sci.* **2005**, *30* (11), 622–629.

(24) Dokmanić, I.; Šikić, M.; Tomić, S. Metals in Proteins: Correlation between the Metal-Ion Type, Coordination Number and the Amino-Acid Residues Involved in the Coordination. *Acta Crystallogr. D Biol. Crystallogr.* **2008**, *64* (3), 257–263.

(25) Ohata, J.; Minus, M. B.; Abernathy, M. E.; Ball, Z. T. Histidine-Directed Arylation/Alkenylation of Backbone N–H Bonds Mediated by Copper(II). *J. Am. Chem. Soc.* **2016**, *138* (24), 7472–7475.

(26) Ohata, J.; Zeng, Y.; Segatori, L.; Ball, Z. T. A Naturally Encoded Dipeptide Handle for Bioorthogonal Chan–Lam Coupling. *Angew. Chem. Int. Ed.* **2018**, *57* (15), 4015–4019.

(27) Waibel, R.; Alberto, R.; Willuda, J.; Finnern, R.; Schibli, R.; Stichelberger, A.; Egli, A.; Abram, U.; Mach, J.-P.; Plückthun, A.; et al. Stable One-Step Technetium-99m Labeling of His-Tagged Recombinant Proteins with a Novel Tc(I)–carbonyl Complex. *Nat. Biotechnol.* **1999**, *17* (9), 897–901.

(28) Kapanidis, A. N.; Ebright, Y. W.; Ebright, R. H. Site-Specific Incorporation of Fluorescent Probes into Protein: Hexahistidine-Tag-Mediated Fluorescent Labeling with (Ni2+:Nitrilotriacetic Acid)N−Fluorochrome Conjugates. *J. Am. Chem. Soc.* **2001**, *123* (48), 12123–12125.

(29) Lata, S.; Gavutis, M.; Tampé, R.; Piehler, J. Specific and Stable Fluorescence Labeling of Histidine-Tagged Proteins for Dissecting Multi-Protein Complex Formation. *J. Am. Chem. Soc.* **2006**, *128* (7), 2365–2372.

(30) Wang, X.; Jia, J.; Huang, Z.; Zhou, M.; Fei, H. Luminescent Peptide Labeling Based on a Histidine-Binding Iridium(III) Complex for Cell Penetration and Intracellular Targeting Studies. *Chem. – Eur. J.* **2011**, *17* (29), 8028–8032.

(31) Lai, Y.-T.; Chang, Y.-Y.; Hu, L.; Yang, Y.; Chao, A.; Du, Z.-Y.; Tanner, J. A.; Chye, M.-L.; Qian, C.; Ng, K.-M.; et al. Rapid Labeling of Intracellular His-Tagged Proteins in Living Cells. *Proc. Natl. Acad. Sci.* **2015**, *112* (10), 2948–2953.

(32) Li, X.; Ma, H.; Dong, S.; Duan, X.; Liang, S. Selective Labeling of Histidine by a Designed Fluorescein-Based Probe. *Talanta* **2004**, *62* (2), 367–371.

(33) Li, X.; Ma, H.; Nie, L.; Sun, M.; Xiong, S. A Novel Fluorescent Probe for Selective Labeling of Histidine. *Anal. Chim. Acta* **2004**, *515* (2), 255–260.

(34) Takaoka, Y.; Tsutsumi, H.; Kasagi, N.; Nakata, E.; Hamachi, I. One-Pot and Sequential Organic Chemistry on an Enzyme Surface to Tether a Fluorescent Probe at the Proximity of the Active Site with Restoring Enzyme Activity. *J. Am. Chem. Soc.* **2006**, *128* (10), 3273–3280.

(35) Wakabayashi, H.; Miyagawa, M.; Koshi, Y.; Takaoka, Y.; Tsukiji, S.; Hamachi, I. Affinity-Labeling-Based Introduction of a Reactive Handle for Natural Protein Modification. *Chem. – Asian J. 3* (7), 1134–1139.

(36) Puttick, J.; Baker, E. N.; Delbaere, L. T. J. Histidine Phosphorylation in Biological Systems. *Biochim. Biophys. Acta BBA - Proteins Proteomics* **2008**, *1784* (1), 100–105.

(37) Besant, P. G.; Attwood, P. V. Detection and Analysis of Protein Histidine Phosphorylation. *Mol. Cell. Biochem.* **2009**, *329* (1–2), 93–106.

(38) Kee, J.-M.; Muir, T. W. Chasing Phosphohistidine, an Elusive Sibling in the Phosphoamino Acid Family. *ACS Chem. Biol.* **2012**, *7* (1), 44–51.

(39) Potel, C. M.; Lin, M.-H.; Heck, A. J. R.; Lemeer, S. Widespread Bacterial Protein Histidine Phosphorylation Revealed by Mass Spectrometry-Based Proteomics. *Nat. Methods* **2018**, *15* (3), 187–190.

(40) Medzihradszky, K. F.; Phillipps, N. J.; Senderowicz, L.; Wang, P.; Turck, C. W. Synthesis and Characterization of Histidine-Phosphorylated Peptides. *Protein Sci. 6* (7), 1405–1411.

(41) Hohenester, U. M.; Ludwig, K.; König, S. Chemical Phosphorylation of Histidine Residues in Proteins Using Potassium Phosphoramidate -- a Tool for the Analysis of Acid-Labile Phosphorylation. *Curr. Drug Deliv.* **2013**, *10* (1), 58–63.

(42) Lasker, M.; Bui, C. D.; Besant, P. G.; Sugawara, K.; Thai, P.; Medzihradszky, G.; Turck, C. W. Protein Histidine Phosphorylation: Increased Stability of Thiophosphohistidine. *Protein Sci. 8* (10), 2177–2185.

(43) Pirrung, M. C.; James, K. D.; Rana, V. S. Thiophosphorylation of Histidine. *J. Org. Chem.* **2000**, *65* (25), 8448–8453.

(44) Ruman, T.; Długopolska, K.; Jurkiewicz, A.; Rut, D.; Frączyk, T.; Cieśla, J.; Leś, A.; Szewczuk, Z.; Rode, W. Thiophosphorylation of Free Amino Acids and Enzyme Protein by Thiophosphoramidate Ions. *Bioorganic Chem.* **2010**, *38* (2), 74–80.

(45) Westheimer, F. H. Why Nature Chose Phosphates. *Science* **1987**, *235* (4793), 1173–1178.

(46) Hong, V.; Presolski, S. I.; Ma, C.; Finn, M. G. Analysis and Optimization of Copper-Catalyzed Azide–Alkyne Cycloaddition for Bioconjugation. *Angew. Chem. Int. Ed. 48* (52), 9879–9883.

Supporting information for

Bioinspired Thiophosphorodichloridate Reagents for Chemoselective Histidine Bioconjugation

Shang Jia[†] and Christopher J. Chang[†‡§*]

†Department of Chemistry, University of California, Berkeley, CA 94720, USA

‡Department of Molecular and Cell Biology, University of California, Berkeley, CA 94720, USA

§Howard Hughes Medical Institute, University of California, Berkeley, CA 94720, USA

Table of contents

Supplementary Figures

Table S1 Stability of TPAC-labelled Fmoc-His-OH Purified TPAC-labelled Fmoc-His-OH (0.5 mM) was treated under the following conditions in water (1−7) or PBS (8−12) and analyzed by HPLC after indicated period of time.

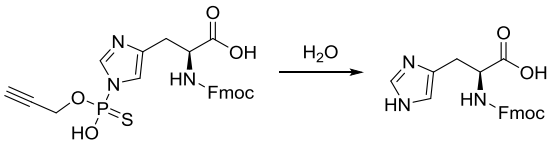

Entry	Additive (concentration)	Temperature / ℃	Time / h	Hydrolysis ratio
1	Formic acid (1 M)	25	1	1%
2	Formic acid (1 M)	25	14	15%
3	HCl (0.2 M)	25	1	<1%
4	HCl (0.2 M)	25	14	20
5	$NH_3 \cdot H_2O$ (1 M)	25	1	<1%
6	$NH_3 \cdot H_2O$ (1 M)	25	14	<1%
7	NaOH (0.2 M)	25	1	n.d.[a]
8	PBS	80	1	2%
9	PBS	80	14	32%
10	TCEP (5 mM)[b]	65	0.5	<1%
11	Dithiothreitol (5 mM)	65	0.5	1%
12	Iodoacetamide (10 mM)	37	1	2%

[a] Fmoc protection group was cleaved during treatment. [b] Tris(2-carboxyethyl)phosphine.

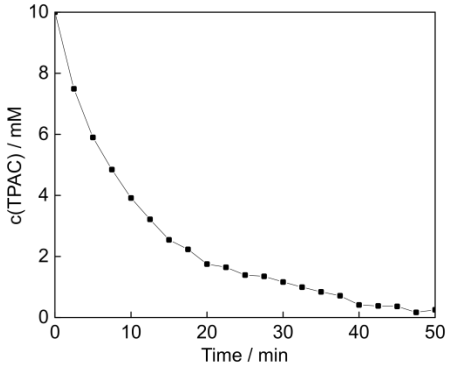

Figure S1 Kinetics of TPAC hydrolysis in phosphate buffered 1:1 D_2O/CD_3CN (100 mM K_3PO_4, adjusted to *p*D 7.0 by *p*H strip), monitored by ^1H NMR.

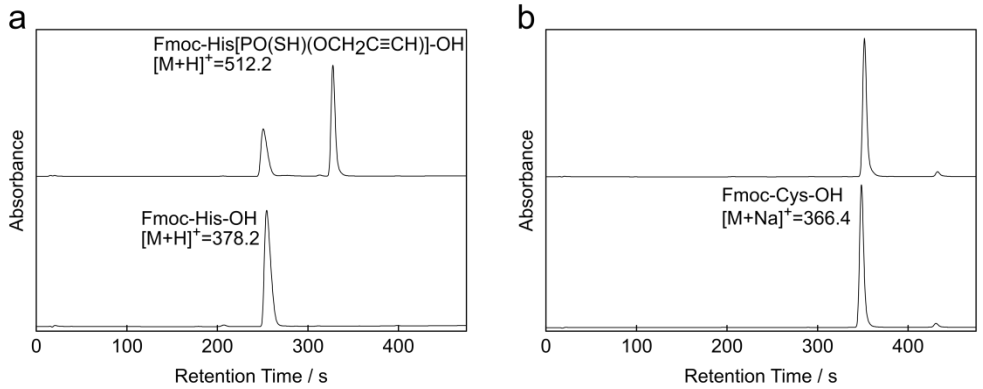

Figure S2 Reactivity of TPAC toward small molecule histidine and cysteine. (a) HPLC chromatograms showing the reactivity of TPAC toward Fmoc-His-OH. Top: reaction mixture of TPAC and Fmoc-His-OH. Bottom: Fmoc-His-OH. (b) HPLC chromatograms showing TPAC is not reactive toward Fmoc-Cys-OH. Top: reaction mixture of TPAC and Fmoc-Cys-OH. Bottom: Fmoc-Cys-OH.

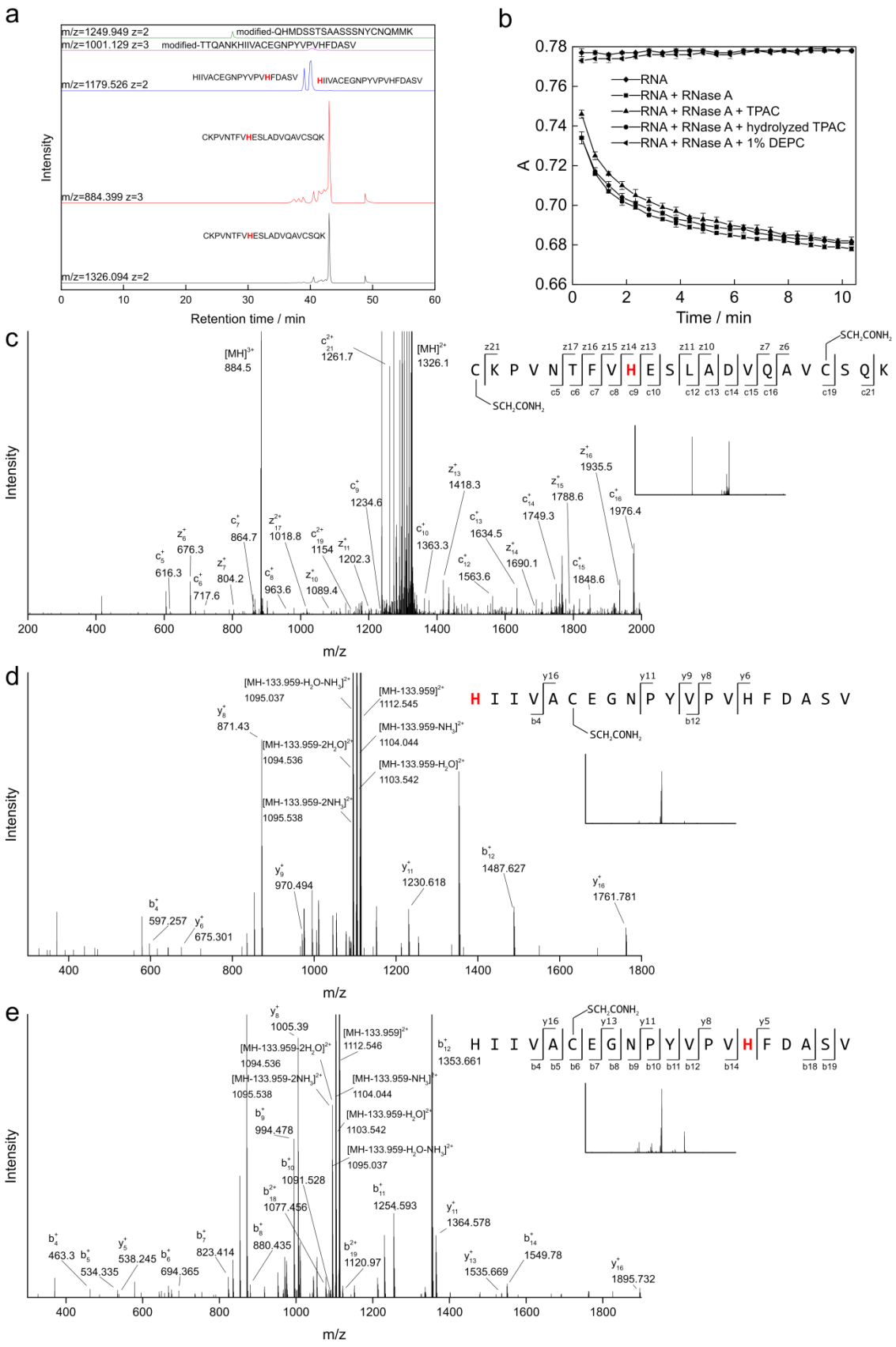
a
m/z=1249.949 z=2
modified-QHMDSSTSAASSSNYCNQMMK
m/z=1001.129 z=3
modified-TTQANKHIIVACEGNPYVPVHFDASV
HIIVACEGNPYVPVHFDASV
m/z=1179.526 z=2
HIIVACEGNPYVPVHFDASV
CKPVNTFVHESLADVQAVCSQK
m/z=884.399 z=3
CKPVNTFVHESLADVQAVCSQK
m/z=1326.094 z=2
Intensity
Retention time / min
b
RNA
RNA + RNase A
RNA + RNase A + TPAC
RNA + RNase A + hydrolyzed TPAC
RNA + RNase A + 1% DEPC
A
Time / min
c
Intensity
m/z
d
Intensity
m/z
e
Intensity
m/z

Figure S3 LC-MS/MS analysis of digested TPAC-labelled ribonuclease A (RNase A). (a) Extracted precursor ion chromatograms of peptides carrying TPAC modification (ΔM=133.959). Identified modification sites by MS2 spectra are highlighted in red. (b) Activity assay shows TPAC does not react much with active site histidine residues on RNase A. RNase A (0.5 mg/mL) was treated with 2 mM TPAC, 2 mM hydrolyzed TPAC or 1% diethylpyrocarbonate (DEPC) before incubating with RNA in 25 mM HEPES buffered at *p*H 8.5. The absorbance of RNA is monitored at 300 nm. (c) ETD MS/MS spectra and (d),(e) CID MS/MS spectrum of major TPAC-modified peptides. Y-axis is zoomed in to show fragment peaks; full spectrum is shown as inset.

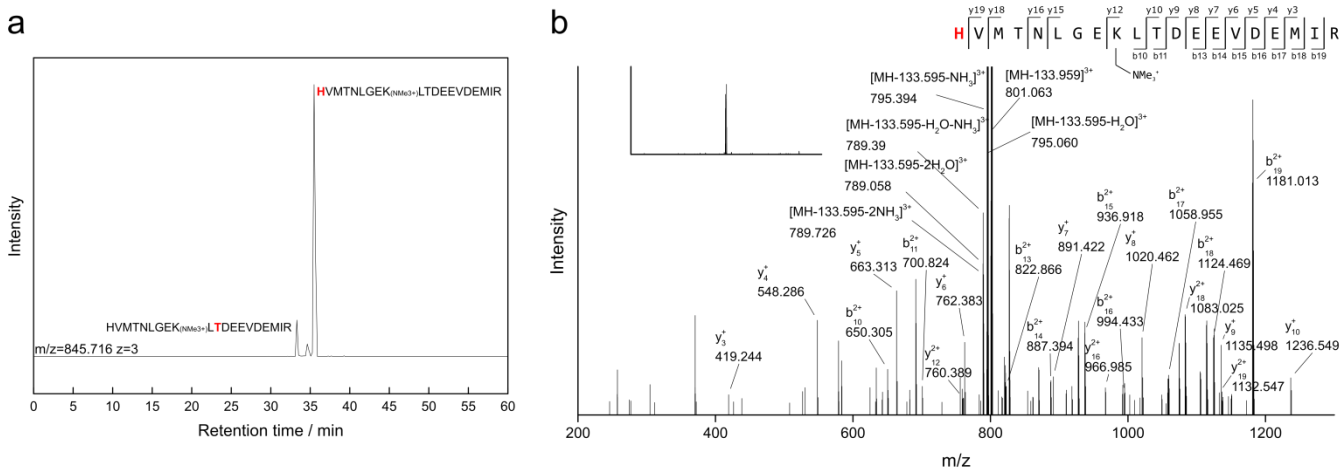

Figure S4 LC-MS/MS analysis of digested TPAC-labelled calmodulin. (a) Extracted precursor ion chromatogram of peptides carrying TPAC modification (ΔM=133.959). Identified modification sites by MS2 spectra are highlighted in red. (b) CID MS/MS spectrum of major TPAC-modified peptide. Y-axis is zoomed in to show fragment peaks; full spectrum is shown as inset.

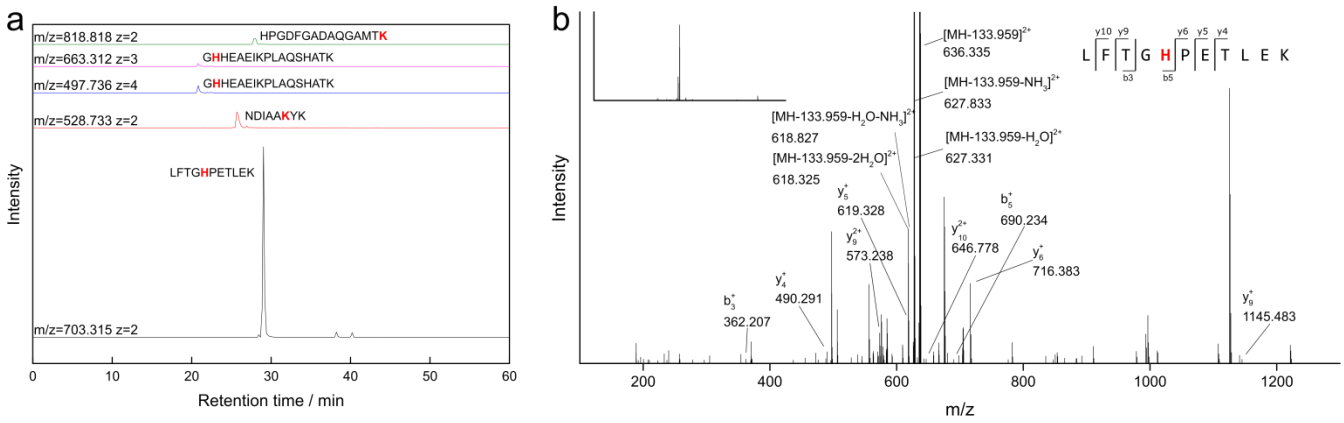

Figure S5 LC-MS/MS analysis of digested TPAC-labelled myoglobin. (a) Extracted precursor ion chromatogram of peptides carrying TPAC modification (ΔM=133.959). Identified modification sites by MS2 spectra are highlighted in red. (b) CID MS/MS spectrum of major TPAC-modified peptide. Y-axis is zoomed in to show fragment peaks; full spectrum is shown as inset.

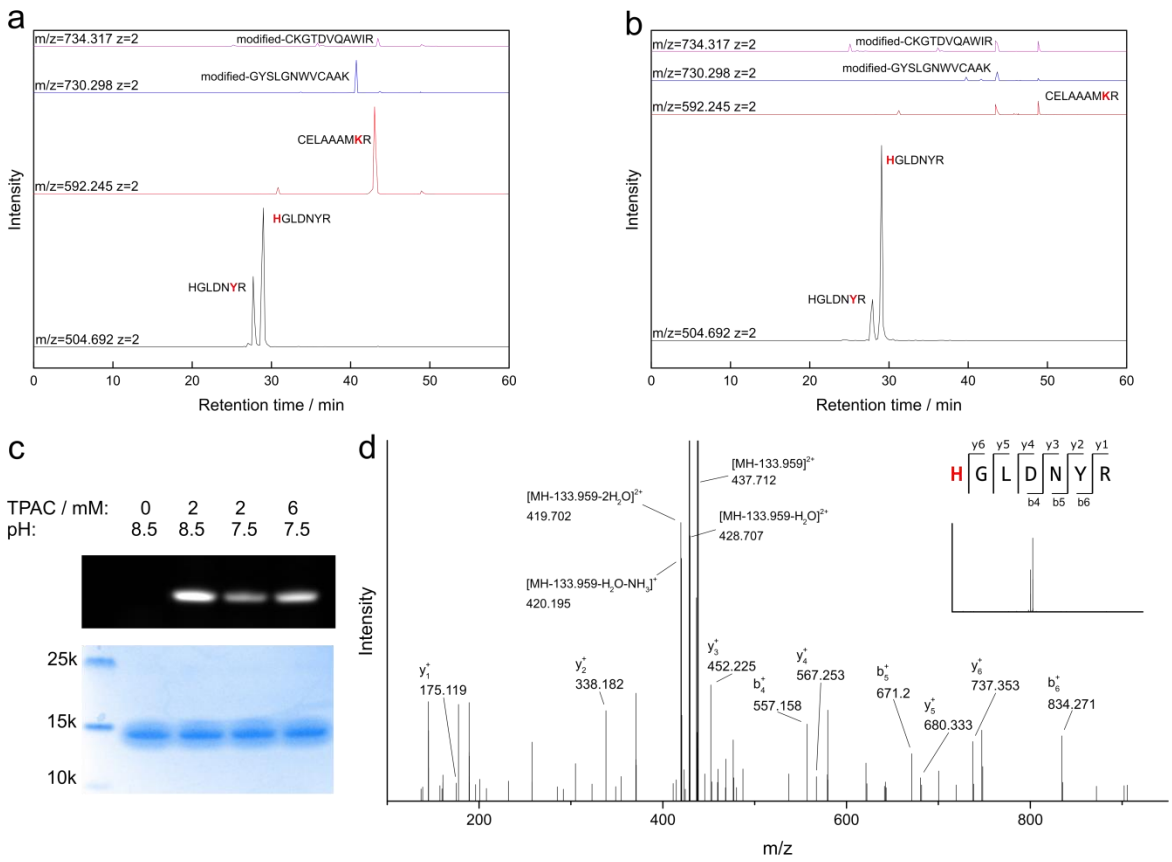

Figure S6 LC-MS/MS analysis of digested TPAC-labelled lysozyme. (a) Extracted precursor ion chromatogram of peptides carrying TPAC modification (ΔM=133.959), digested from lysozyme treated with 2mM TPAC at *p*H 8.5. (b) Extracted precursor ion chromatogram of peptides carrying TPAC modification (ΔM=133.959), digested from lysozyme treated with 6 mM TPAC at *p*H 7.5. Modification sites identified by MS2 spectra are highlighted in red. (c) In-gel fluorescence shows comparable labeling efficiency between these two conditions. Lysozyme was labelled with TPAC, conjugated with Cy3-N_3 by CuAAC and subject to SDS-PAGE. Top: fluorescence. Bottom: coomassie. (d) CID MS/MS spectrum of major TPAC-modified peptide. Y-axis is zoomed in to show fragment peaks; full spectrum is shown as inset.

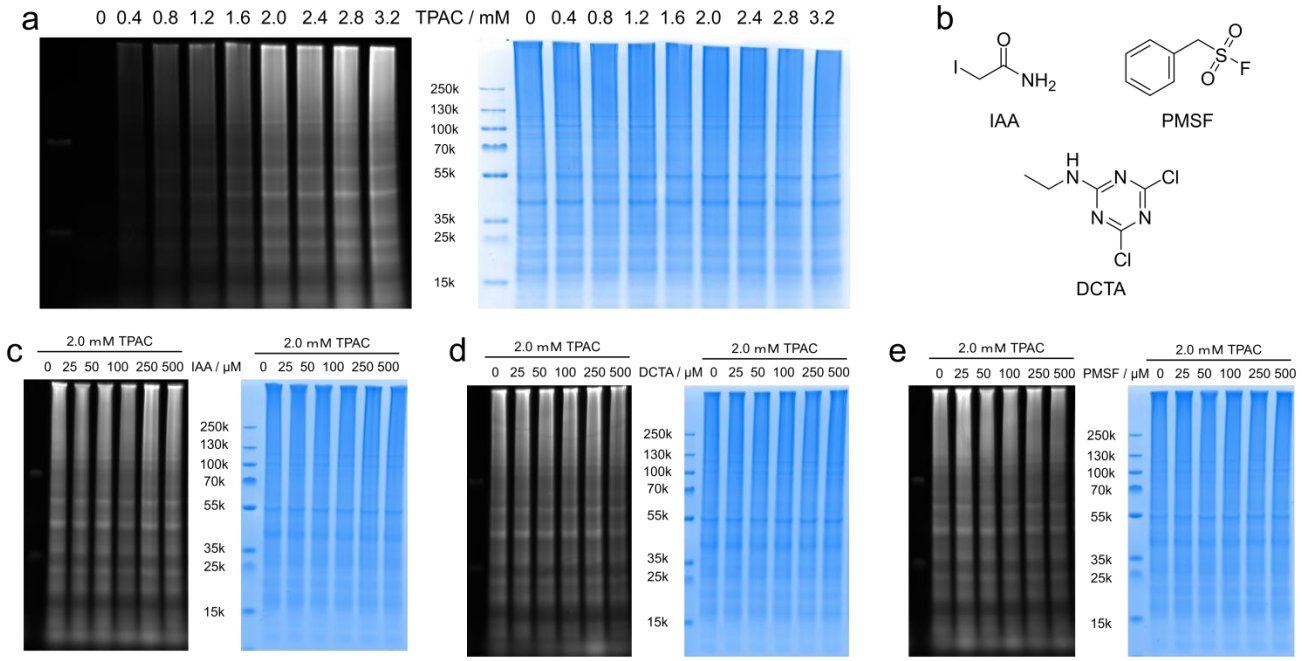

Figure S7 Labeling of HeLa lysate with TPAC in 50 mM HEPES buffer, *p*H 7.5. (a) Dose-dependent labeling of HeLa proteome with TPAC. Lysates were treated with indicated concentration of TPAC and subsequently conjugated with Cy3-N_3 by CuAAC and analyzed by SDS-PAGE. Left: fluorescence. Right: coomassie. (b) Structures of competing electrophiles: IAA that reacts with cysteine, PMSF that reacts with reactive serine, and DCTA that reacts with lysine. HeLa lysates were pretreated for 1 h with (c) IAA, (d) DCTA and (e) PMSF prior to TPAC labeling; the labelled lysates were subsequently conjugated with Cy3-azide by CuAAC and analyzed by SDS-PAGE. Left: fluorescence. Right: coomassie.

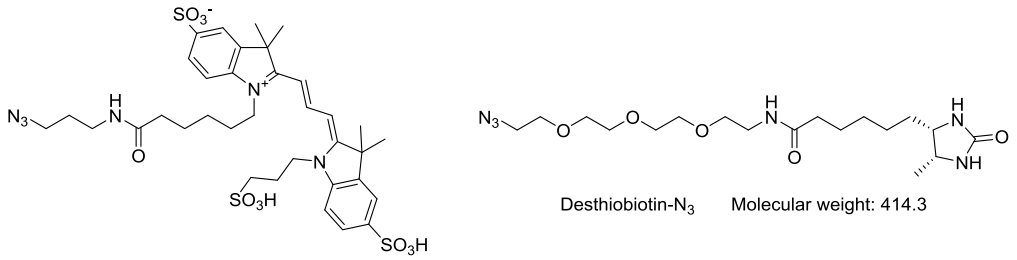

Figure S8 Structure and molecular weight of model azide compounds: Cy3-N_3 and desthiobiotin-N_3.

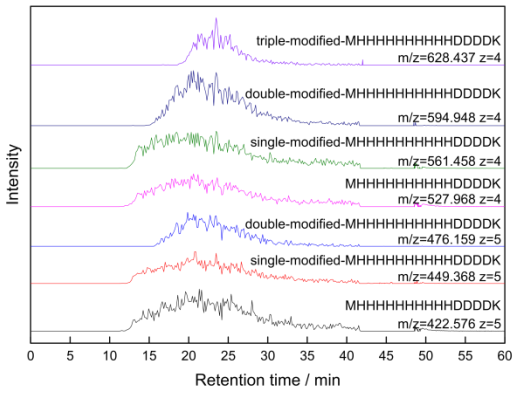

Figure S9 Extracted precursor ion chromatogram of His-tag peptide and major peptides carrying TPAC modification (ΔM=133.959), digested from His-tagged GFP treated with 2mM TPAC at *p*H 8.5. For simplicity, peptides with N-terminal methionine excised and peptides with oxidized methionine are not shown.

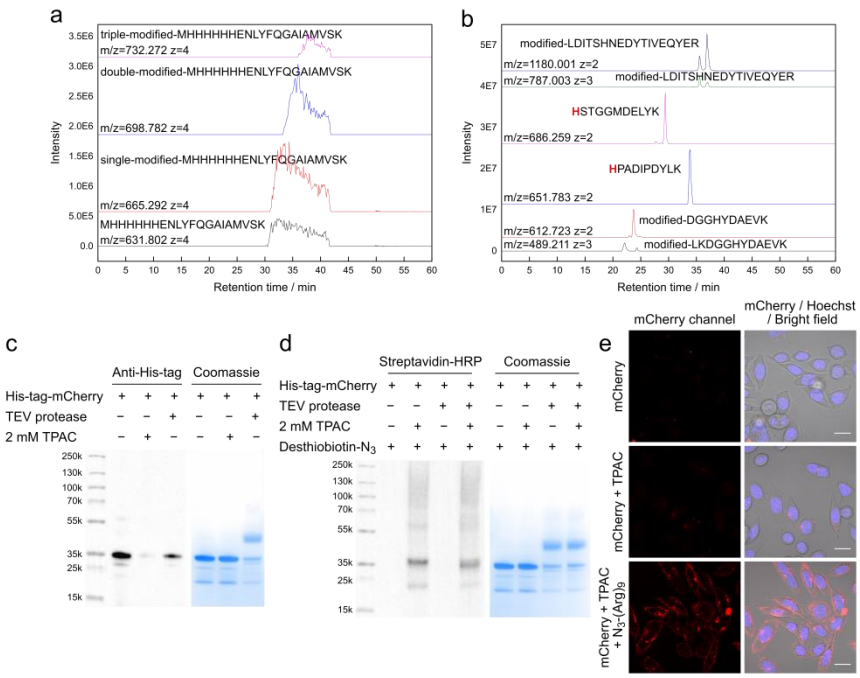

Figure S10 Functionalization of His-tag on mCherry to enable protein delivery. (a) Extracted precursor ion chromatogram of unmodified and TPAC-modified (ΔM=133.959) His-tag peptides, digested from His-tagged GFP treated with 2mM TPAC at *p*H 8.5. (b) Extracted precursor ion chromatogram of other major TPAC-modified peptides. (c) Western blot and coomassie stain showing that labelling of TPAC with His-tagged mCherry significantly reduces its detection by His-tag antibody. TEV protease was used to cleave off His-tag on this protein for comparison. Cleavage of His-tag leads to less coomassie staining but with similar migration on SDS-PAGE (Figure S11b). (d) Streptavidin-HRP blot and coomassie stain showing that removal of the His-tag reduces the labeling by TPAC. His-tagged mCherry and native mCherry prepared by TEV protease cleavage of His-tag were treated with TPAC, followed by CuAAC with desthiobiotin-N_3 and gel-analysis. (e) Transduction of functionilized mCherry into live HeLa cells. Cells were incubated with mCherry (0.1 μg/μL), stained with Hoechst 33342 and imaged. Scale-bars: 20 μm.

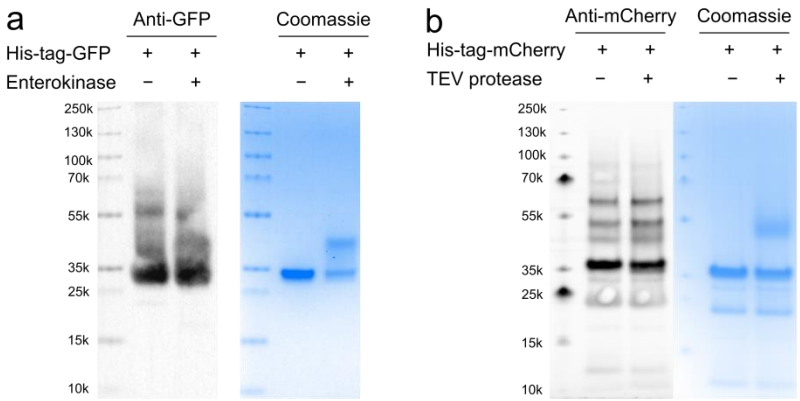

Figure S11 Western blot and coomassie stain of GFP and mCherry. (a) His-tagged GFP and GFP. (b) His-tagged mCherry and mCherry.

Procedures and Characterization Methods

Analysis methods

Reactions on protected amino acid were analyzed by LC/MS using 1220 Infinity LC (Agilent, Santa Clara CA) coupled with Expression-L Compact Mass Spectrometer (Advion, Ithaca NY). Reaction mixtures with single protected amino acid were separated on a Zorbax rapid resolution cartridge (Agilent). Mixtures with multiple protected amino acids were separated on a Zorbax SB-phenyl column (Agilent, 4.6 × 250 mm, 5 μm). Solvent A was water + 0.05% formic acid and solvent B was methanol + 0.05% formic acid. The linear gradient employed for single protected amino acid was 25-100% B in 6.5 min and 100% B for 1.5 min; for multiple amino acids mixture was 45-100% B in 30 min and 100% B for 10 min.

Intact protein samples were analyzed using a Synapt G2-Si mass spectrometer equipped with an ionKey ESI source (Protein ionKey, C4, 1.7 μm, 0.150 × 50 mm, 300 Å), operated in the positive ion mode, and connected in line with an Acquity M-class LC system (Waters, Milford MA). This instrumentation is located in the QB3/Chemistry Mass Spectrometry Facility at the University of California, Berkeley. The obtained mass spectra were deconvoluted using UniDec.[1]

Proteolytically digested protein samples were analyzed using an LTQ-Orbitrap-XL mass spectrometer equipped with an electrospray ionization (ESI) source, operated in the positive ion mode, and connected in line with an UltiMate3000 RSLCnano liquid chromatography (LC) system (Thermo Fisher). The LC system was equipped with a reversed-phase analytical column (Acclaim PepMap100, C18, 3 μm, 0.075 × 250 mm, 100 Å, Thermo Fisher). The obtained data were processed with Trans-Proteomic Pipeline using the Comet search algorism (Institute for Systems Biology, Seattle WA).[2] The MS2 spectra were annotated with a mass tolerance of 15 ppm. The extracted-ion chromatograms (XIC) of MS1 were

generated from the .ms1 file from RawConverter, using an in-house script that picks correctly-charged precursor ions with a mass tolerance of 20 ppm.

Enzymatic digestion of TPAC-labelled protein for LC-MS/MS analysis

Protein (0.5 mg/mL) was labelled with 2 mM TPAC following the general procedure unless otherwise noted. Labelled protein was precipitated by acetone to remove excess TPAC. The pellet was dissolved in 25 mM HEPES, *p*H 8.0 containing 6 M urea and subject to reduction (TCEP, 5 mM, 20 min) and alkylation (iodoacetamide, 10 mM, 40 min at 37 ℃). Protein was precipitated again by acetone, suspended in 25 mM HEPES, *p*H 8.0 and digested by trypsin (1:20, Promega, Madison WI) overnight at 37 ℃.

Synthesis of phosphorus electrophiles and related chemicals

Synthetic materials and methods

Unless otherwise noted, all commercial reagents were used without further purification. All reactions utilizing air- or moisture-sensitive reagents were performed in dried glassware under an atmosphere of dry N_2. THF used for anhydrous reactions was dried and stored over 4 Å molecular sieves. 2-Azidoethanol [3] and succinimidyl 3-azidopropanoate [4] were synthesized according to literature procedure. 3-Azidopropanoic acid was purchased from Click Chemistry Tools. H-$(Arg)_9$-OH trifluoroacetate salt was purchased from Bachem (Bubendorf, Switzerland). All other reagents were purchased from Sigma-Aldrich. ^{1}H NMR, ^{13}C NMR and ^{31}P NMR spectra were collected in $CDCl_3$, MeOD or acetone (Cambridge Isotope Laboratories, Cambridge MA) at 25 ℃ on AVB-400, AVQ-400 or AV-600 spectrometers at the College of Chemistry NMR Facility at the University of California, Berkeley. All chemical shifts in ^{1}H NMR and ^{13}C NMR are reported in the standard δ notation of ppm relative to residual solvent peak ($CDCl_3$ δH=7.26, δC=77.16; MeOD δH=3.31, δC=49.00; acetone: δH=2.05, δC=29.84), and for ^{31}P NMR 85% phosphoric acid in sealed capillary tube is used as internal standard (δP=0.00). Splitting patterns are indicated as follows: s, singlet; d, doublet; t, triplet; q, quartet; m, multiplet; br, broad. Low resolution election ionization mass spectral analysis was carried out using Agilent 5975C 7890A GC/MS System. High resolution mass spectral analysis (ESI-MS and APCI-MS) were carried out at LBNL Catalysis Facility at the Lawrence Berkeley National Laboratory (Berkeley Lab) using PerkinElmer AxION® 2 TOF MS.

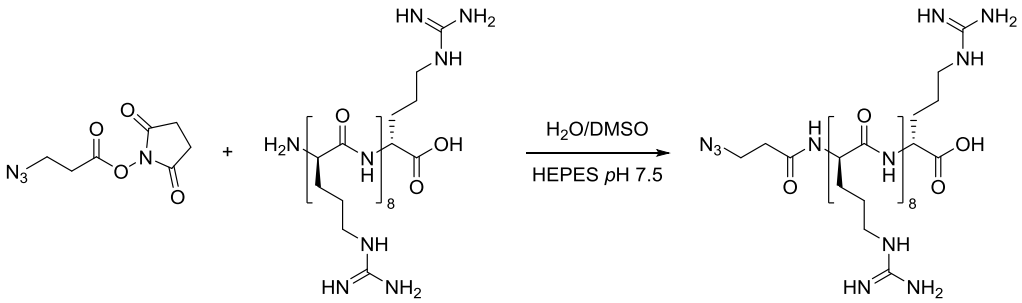

3-Azidoacetyl-(Arg)$_9$-OH. H-(Arg)$_9$-OH trifluoroacetate salt (1 mg, approx. 0.5 μmol) was dissolved in 400 μL H_2O in an Eppendorf tube. To this solution was added HEPES buffer (100 μL, 50 mM *p*H=7.5) and succinimidyl 3-azidopropanoate (2.54 mg, 12 μmol) in DMSO (500 μL). The solution was mixed thoroughly and reacted in the dark for 3 h. The solution was then loaded onto a strong cation exchange spin column (Thermo Fisher). The column was washed with 25 mM ammonium acetate (2×400 μL) and eluted with 2 M ammonium acetate. The eluent was concentrated in a vacuum chamber overnight, and the residue was dissolved in water to a final volume of 50 μL to give an approx. 10 mM stock solution. HRMS (ESI$^+$) m/z calcd 507.6567, found 507.6502 for $C_{57}H_{116}N_{39}O_{11}^{3+}$ (M+3H$^+$); calcd 514.9840, found 514.9745 for $C_{57}H_{115}N_{39}NaO_{11}^{3+}$ (M+2H$^+$+Na$^+$).

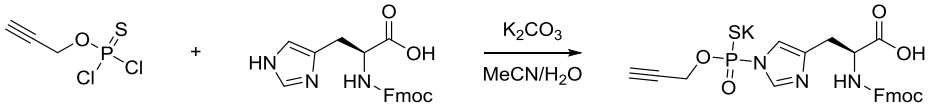

Potassium *O*-propargyl (*N*^{2}-Fmoc-L-histidino)thiophosphate. Fmoc-His-OH (0.20 g, 0.53 mmol) and K_2CO_3 (1.1 g, 8.0 mmol) was dissolved in 4:6 H_2O/MeCN (15 mL). To this mixture was added TPAC (0.30 g, 1.6 mmol) in MeCN (5 mL) over 1 h under vigorous stirring. The mixture was further stirred for 2 h and the desired product was separated by RP-HPLC to give the product as an off-white solid (0.22 g, 75%). This compound has the same retention time and m/z on LC/MS as the product in Figure S2a. ^{1}H NMR (400 MHz, MeOD) δ 8.87 (s, 1H), 7.78 (d, *J* = 7.4 Hz, 2H), 7.63 (d, *J* = 7.2 Hz, 2H), 7.49 (s, 1H), 7.34 (dt, *J* = 28.2, 7.3 Hz, 4H), 4.68 – 4.58 (m, 2H), 4.51 (dd, *J* = 9.3, 4.8 Hz, 1H), 4.37 – 4.28 (m, 2H), 4.20 (t, *J* = 6.7 Hz, 1H), 3.27 (d, *J* = 4.7 Hz, 1H), 3.09 (dd, *J* = 15.1, 9.7 Hz, 1H), 2.76 – 2.66 (m, 1H). ^{31}P NMR (162 MHz, MeOD) δ 49.01. HRMS (ESI$^+$) m/z calcd 512.1040, found 512.1092 for $C_{24}H_{23}N_3O_6PS^+$ (M+H$^+$).

NMR Spectra

^{1}H NMR of TPAC ($CDCl_3$, 400 MHz)

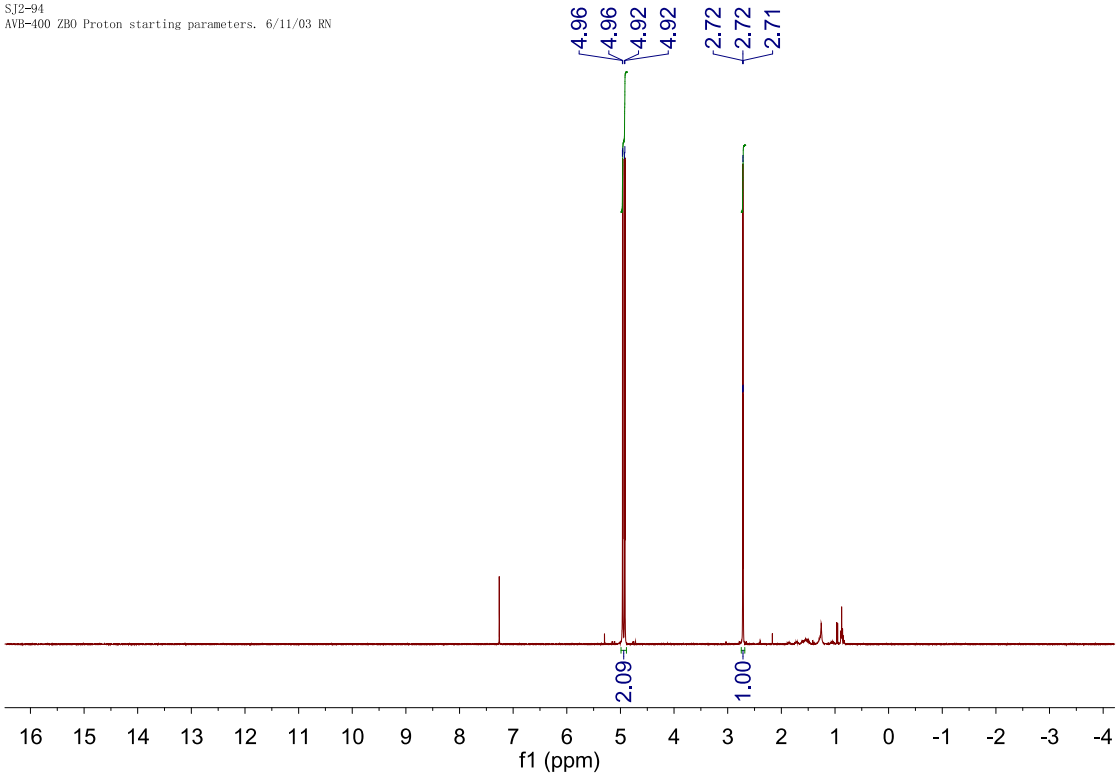

^{13}C NMR of TPAC ($CDCl_3$, 101 MHz)

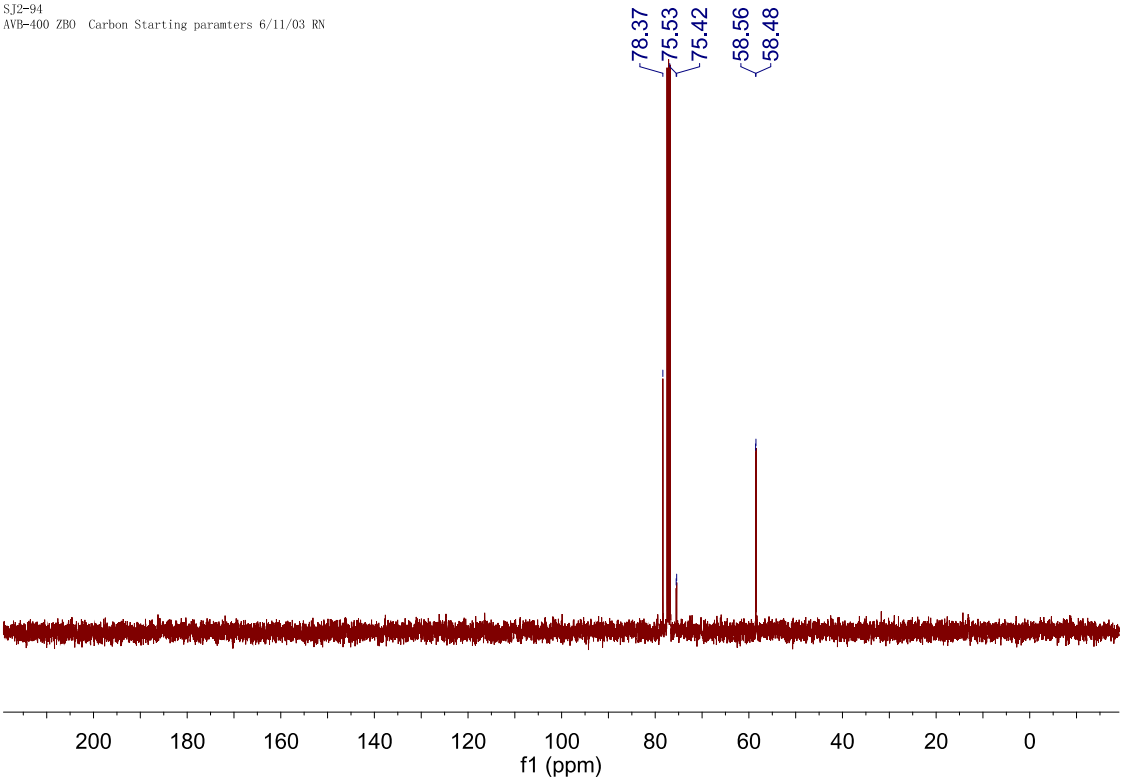

^{31}P NMR ($CDCl_3$, 162 MHz)

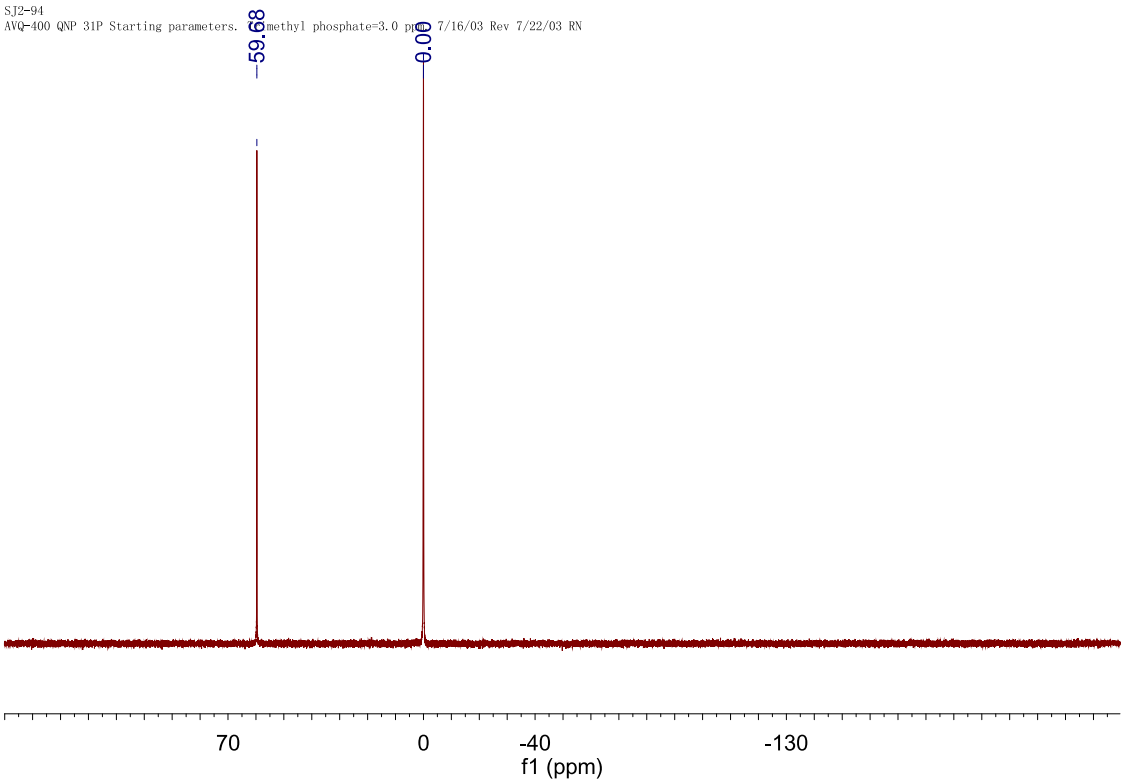

References

(1) Marty, M. T.; Baldwin, A. J.; Marklund, E. G.; Hochberg, G. K. A.; Benesch, J. L. P.; Robinson, C. V. Bayesian Deconvolution of Mass and Ion Mobility Spectra: From Binary Interactions to Polydisperse Ensembles. *Anal. Chem.* **2015**, *87* (8), 4370–4376.

(2) Eng, J. K.; Jahan, T. A.; Hoopmann, M. R. Comet: An Open-Source MS/MS Sequence Database Search Tool. *PROTEOMICS 13* (1), 22–24.

(3) Hounsou, C.; Margathe, J.-F.; Oueslati, N.; Belhocine, A.; Dupuis, E.; Thomas, C.; Mann, A.; Ilien, B.; Rognan, D.; Trinquet, E.; et al. Time-Resolved FRET Binding Assay to Investigate Hetero-Oligomer Binding Properties: Proof of Concept with Dopamine D1/D3 Heterodimer. *ACS Chem. Biol.* **2015**, *10* (2), 466–474.

(4) Grandjean, C.; Boutonnier, A.; Guerreiro, C.; Fournier, J.-M.; Mulard, L. A. On the Preparation of Carbohydrate−Protein Conjugates Using the Traceless Staudinger Ligation. *J. Org. Chem.* **2005**, *70* (18), 7123–7132.